Environmental Engineering and Management Journal

August 2019, Vol. 18, No. 8, 1765-1772
http://www.eemj.icpm.tuiasi.ro/; http://www.eemj.eu

"Gheorghe Asachi" Technical University of Iasi, Romania

HETEROSTRUCTURES OF SILVER AND ZINC BASED LAYERED DOUBLE HYDROXIDES FOR POLLUTANT REMOVAL UNDER SIMULATED SOLAR LIGHT

Diana Gilea[1], Doina Lutic[2], Gabriela Carja[1]*

[1]"Gheorghe Asachi" Technical University of Iasi, "Cristofor Simionescu"Faculty of Chemical Engineering and Environmental Protection, 73 Prof. D. Mangeron Blvd., Iasi, Romania,
[2] Al. I. Cuza University of Iasi, Faculty of Chemistry, 11 Carol I Blvd., 700506 Iasi, Romania

Abstract

Nitrophenols are among the most hazardous refractory pollutants showing high stability and solubility in water. This work presents heterostructures of nanoparticles of silver/zinc based layered double hydroxides as efficient photocatalysts for degrading 4-nitrophenol (4-NPh), from aqueous solutions under irradiation with solar light. ZnAl-layered double hydroxides (ZnAl-LDHs) with Zn/Al = 2:1 and Zn/Al = 3:1 ratios were synthesized, characterized by XRD, FTIR, SEM and TEM and further used as precursors to form mixed oxides after calcination at 550°C. Based on the capability of the calcined LDHs to reconstruct their layered structure in aqueous media, $AgNO_3$ solutions were used to obtain Ag nanoparticles directly on ZnAl-LDHs matrices. The calculated value of the band gap of Ag/ZnAl-LDHs was ~ 3.1 eV, revealing that these materials might successfully act as photocatalysts under solar light irradiation. The photocatalytic tests performed on the decomposition of 4-NPh aqueous solutions indicate that on Ag/ZnAl-LDH (3:1)87% of 4-NPh was degraded after 6 h under irradiation with solar light.

Key words: solar photocatalysis, layered double hydroxides, silver nanoparticles, 4-nitrophenol

Received: September, 2018; Revised final: January, 2019; Accepted: April, 2019; Published in final edited form: April, 2019

1. Introduction

Nitrophenols are toxic and bio-refractory pollutants with a negative impact on human health. Nowadays, nitrophenols are used in the production of pesticides, as insecticides and herbicides, as well as in the production of many synthetic dyes. Hence, 4-NPh is a common pollutant that has been found in natural and industrial wastewaters. A few studies have reported the degradation of 4-NPh using solar light photocatalysis (Bora and Mewada, 2017). A photocatalyst is, usually, a material with semiconductor properties able to capture the photon energy and induce the electron jump from the valence band to the conduction band, followed by the generation of HO· radicals, which promote the degradation of the species adsorbed on the solid surface. The method is more economical when the activation of the photocatalyst can be achieved using solar light (Gilea et al., 2018). The solar light consists of a wide majority of visible radiation and about 3% UV radiation. The wavelength of 400 nm (the limit between UV and visible range) corresponds to a band gap value of about 3.1 eV. The large availability of solar light supports the consistent interest of the scientific media and economists for finding convenient materials able to capture and use the solar energy. Titanium dioxide, alone or in many sorts of mixtures with other oxides, eventually doped with transition metals of noble metals is the most investigated semiconductor used as a photocatalyst nowadays (Khaki et al., 2018). However, its large band gap induces restrictions under solar light irradiation.

* Author to whom all correspondence should be addressed: e-mail: carja@uaic.ro; Phone: +40(232)278683

Layered double hydroxides (LDHs) are good candidates to replace TiO_2 catalyst. LDHs might contains, among the divalent and trivalent ionic species, semiconductor oxides such that ZnO, SnO_2, In_2O_3, Ga_2O_3 (Carja et al., 2017). Moreover, the LDHs structure can be transformed by calcination to mixtures of mixed oxides and then restored by the reconstruction processes. The transformation of the mixed oxides to reconstruct again the layered double hydroxides network is known as LDHs "structural memory effect" (Klemkaite et al., 2001). The LDHs reconstructed in the metal salts aqueous solutions contains in the interlayers the anions of the solutions (Carja et al., 2017; Mishra et al., 2018; Zhao et al., 2010).

Plasmonic metals (Ag, Au, Pt, Pd, etc.) have also been successfully deposited on layered double hydroxides, giving rise to active photocatalysts (Katsumata et al., 2013). The silver nanoparticles deposited on the various oxide supports have attracted attention due to their interesting light-responsive properties. The co-assemblies of ZnAl-LDH and nano-sized Ag might join the properties of the components and increase the photocatalytic response under solar light exposure (Chen et al., 2012; Gilea et al., 2018).

This work presents nanoarchitectonics of Ag/ZnAl-LDHs with LDHs with Zn/Al atomic ratios of 2/1 and 3/1 as novel solar light responsive photocatalysts for the degradation of 4-NPh from aqueous solutions, using solar light irradiation. The catalysts were obtained by the reconstruction of the mixed oxides that resulted after the calcination of ZnAl-LDHs in $AgNO_3$ aqueous solution, at room temperature. No surfactants were used fduring the catalysts fabrication. During the re-formation of the layered structure of the LDHs, Ag cations from the $AgNO_3$ solution were organized as Ag nanoparticles deposited on the surface of the LDHs platelets (Gilea et al., 2018; Seftel et al., 2015). This method gives rise to heterostructuring effects, thus contributes to slowing down the surface-bulk charge carrier recombination and maximize the photocatalytic potential (Girish Kumar and Koteswara Rao, 2015).

The obtained catalysts were characterized by physical-chemical techniques and tested in the photocatalytic degradation of 4-NPh under simulated solar light. Results show that undoped ZnAl-LDHs had no photocatalytic response for 4-NPh degradation in aqueous media, while Ag/ZnAl-LDHs heterostructures are active photocatalysts under solar light.

2. Experimental

2.1. Catalysts synthesis

ZnAlLDHs with Zn/Al molar ratios of 2 and 3 were prepared by the coprecipitation method at low supersaturation, at a constant pH value of 8.5, by using 2M aqueous NaOH solution and Na_2CO_3 (Sigma-Aldrich) as precipitation agents (Bîrsanu et al., 2013). The solutions of $Zn(NO_3)_2 \cdot 6H_2O$ (> 98% Sigma Aldrich) and $Al(NO_3)_3 \cdot 9H_2O$ (98% Sigma-Aldrich), were mixed to give an overall salts concentration of 1M, at molar ratios of Zn/Al= 2/1 and 3/1, respectively. Under vigorous magnetical stirring, the addition of NaOH solution was regulated to keep the pH at the desired value, while the nitrates mixture was poured at a flow rate of 1 mL min^{-1}. The resulted precipitates were aged about 24 h at room temperature, separated by filtration, washed several times with distilled water, dried at 80°C in an oven overnight and denoted as Ag/ZnAl-LDH (2:1) and Ag/ZnAl-LDH (3:1).. Then, the solids were calcined at 550°C (10°C min^{-1}) for 7 hours. This temperature value is suitable to transform the LDHs in homogeneous mixtures of oxides (Carja et al., 2015; Elhalil et a., 2018; Rocha et al., 1999). Finally, the resulted mixed oxides were stirred for 12 h in $AgNO_3$ (Sigma Aldrich>99%) (0.1 mol L^{-1}), separated by filtration and dried at 70°C, under vacuum. Further some of the catalysts were calcined at 750°C for 8 hours.

2.2. Catalysts characterization

The structural characterization was performed by XRD, FT-IR spectroscopy, thermal analysis, TEM and SEM analyses. The XRD patterns were obtained on a Shimadzu D6000 apparatus, in the range 10–80° (2 theta), under CuK_α radiation (λ = 1.5406 Å). Transmission electron microscopy (TEM) imaging was performed on a Hitachi H-900 transmission electron microscope operating at an accelerating voltage of 200 kV, coupled with an energy dispersive X-ray (EDX) spectrometer. The FTIR spectra were obtained on KBr pellets using a PerkinElmer Spectrum 100 spectrophotometer (450–4000 cm^{-1}, resolution of 4 cm^{-1}). The UV-DR spectra were recorded on MgO-based pellets.

2.3. Experimental set-up for the catalytic tests

The photocatalytic activity was tested in the photodegradation of 4-nitrophenol from aqueous solutions. The initial concentration of 4-NPh was 0.025 g L^{-1}. A dose of 1 g L^{-1} of photocatalyst was used in the photocatalytic experiments. Before the photocatalytic run, the solid powder dispersed in the solution was stirred in dark for one hour, to allow reaching the adsorption–desorption equilibrium between the solid surface and the adsorbate molecules. Afterwards, the slurries were irradiated in an Unnasol US800 solar simulator (180 W) equipped with UV and visible light block filters under simulated solar light. The reactions were carried out in a 200 mL reactor with water recycling to avoid the evaporation and keep constant the volume and temperature values. Samples of about 4 mL were withdrawn from the reactor after 2, 5, 10, 15, 20, 30, 40, 50, 60 min, then each 30 minutes up to 6 hours from the beginning of the photocatalytic run. The photodegradation profiles were highlighted by tracing the UV-vis absorption spectra on a Jasco V-550 spectrophotometer and

measuring the absorbance at the characteristic wavelength of 399 nm. The conversion values of 4-NPh (X) was calculated on the basis of the absorbance values at time zero (A_o) and the absorbance value at time t (A_t), by the equation (Eq. 1):

$$X = 100 * (A_o - A_t) / A_g \quad (1)$$

3. Results and discussions

3.1. Characterization of the samples

The calcination at 550°C of the as-synthesized samples gave rise to a blend of oxidic compounds, as shown by the patterns in Fig. 1. This temperature value as chosen in order to crash the LDH structure, but still mild to allow the subsequent reconstruction (Carja et al., 2015; Elhalil et a., 2018; Rocha et al., 1999). The main peaks are due to zinc oxide and appear at 31.0; 34.7; 36.4; 47.1; 56.7 and 63.1° (2 theta), respectively, due to the (100), (002), (101), (102), (110), (103) planes of ZnO (Akhtar et al., 2012). The peaks from 38.2; 44.3 and 64.5° might be indexed to the metallic Ag reflections of (111), (200) and (222) planes (Waterhouse et al., 2001). Further the reflections at 31.4° and 34.3° correspond to zinc aluminate $ZnAl_2O_4$ (220) and (311) planes (Sharma et al., 2014), while the peaks from 28 and 35.1° can be due to (012) and (104) planes of bohemite-type alumina (Boumaza et al., 2009; Sharma and Ghose, 2014).

The treatment of the mixed oxides phases with silver nitrate solution was performed to achieve the LDHs reconstruction process.

The success of the operation was confirmed by the presence of some characteristic peaks of LDH structure (see Fig. 2), with reflections at 12.3; 23.7; 34.7; 39.3; 46.8; 60.4 and 61.7°, due to the (003), (006), (009), (015), (018), (110) and (113) planes from the lamellar LDH structure with NO_3^- anions in the interlayer (Seftel et al., 2013).

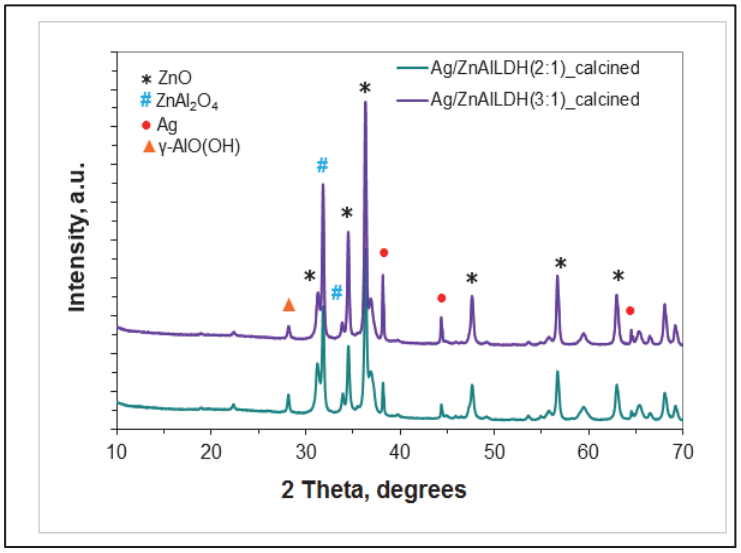

Fig. 1. XRD patterns of the catalysts calcined at 750°C.

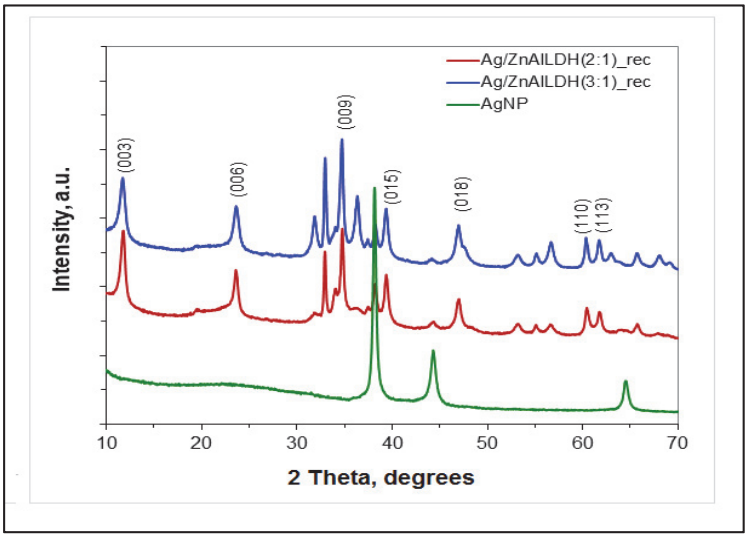

Fig. 2. XRD patterns of the tested Ag/ZnAl-LDHs and Ag nanoparticles.

The FTIR spectra of ZnAl-LDH (2:1) and of the reconstructed LDHs are shown in Fig. 3. The wide and intense band between 3600-3300 cm^{-1}, with a maximum at 3430 cm^{-1} is common for all three samples and is a characteristic of the O – H bond strethcing. In the range 1600 – 400 cm^{-1}, there are not distinctive features between the ZnAl-LDH and Ag/ZnAl-LDH (2:1) and Ag/ZnAl-LDH (3:1). The behavior of the catalysts is similar and is not influenced by the different molar ratio of Zn/Al. The band from 1620 cm^{-1} is due to ν(OH) and ν (H_2O) bands (Balcomb et al., 2015). The sharp band at 1118 cm^{-1} is due to the stretching mode of the carbonate ions.

The peaks from 618 and 427 cm^{-1} are assigned to the presence of M-O vibrations and M-O-H bending. The peaks of 427, 619 and 1118 cm^{-1} are characteristic for the LDH structure containing of CO_3^{2-} ions, coming from the atmospheric carbon dioxide during the reconstruction (Xu et al., 2006; Valcheva–Traykova et al., 1993). The peak at 552 cm^{-1} might also reveal the presence of Ag in the lattice as Ag_2O (Rafiq et al., 2013).

The SEM and TEM images, shown in Fig. 4 (a-b), indicate that the sample consists of relatively uniform LDH-plate-like particles with an average diameter of 120 nm. The TEM image shows small dark points indicating that after the reconstruction, small nanoparticles are deposited on the surface of the large LDHs particles. Joining together the XRD and TEM results, the small NPs might be identified as nanoparticles of Ag^0. Hence, the results of XRD, TEM and SEM analyses together reveal the formation of a complex nanoarchitecture, defined by the joined nanoparticles of Ag and ZnAl-LDH matrices. The average diameter of the AgNP is of the order of 7 nm and they are uniformly distributed on the large plate-like particles of the zinc-based LDHs.

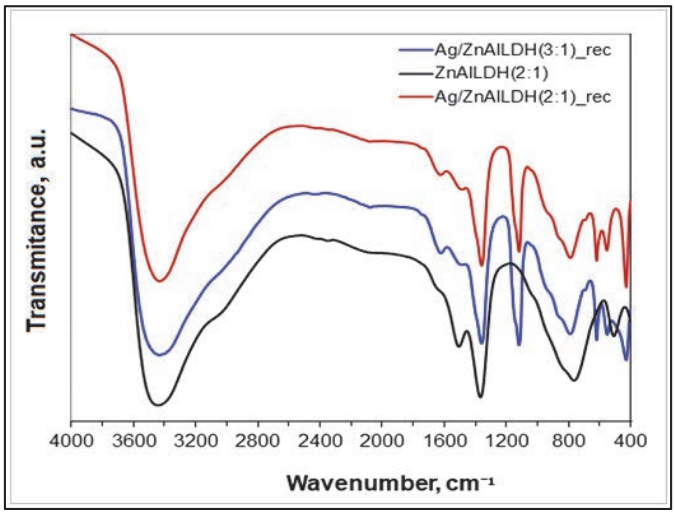

Fig. 3. The FTIR spectra of ZnAl-LDH (2:1) and the tested catalysts.

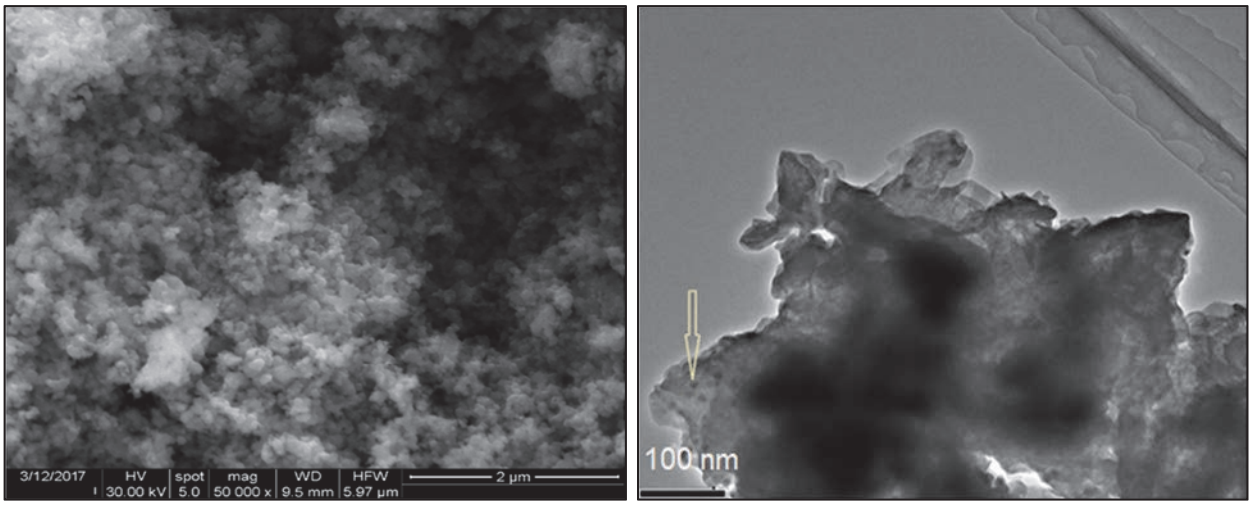

(a) (b)

Fig. 4. (a) SEM of Ag/ZnAl-LDH (2:1), (b) TEM of Ag/ZnAl-LDH (3:1)

Thermal analysis results are shown in Fig. 5(a) for Ag/ZnAl-LDH (2:1) and Fig. 5 (b) for Ag/ZnAl-LDH (3:1). The TG/DTG results show that the behavior is typical for the LDH-type structure. Two distinctive features are observed during the thermal transformations. A decrease of ~ 23 % occurs in two steps up to 400ºC, corresponding to the elimination of the interlayer weakly bonded water up to 209-214ºC and to the subsequent decomposition of the hydroxyl groups from the brucite layer.

Some minor mass losses ~ 3.41%, that occur between 400-800ºC, are assigned to the decomposition of carbonate and nitrate anions accommodated in the LDHs interlayers. The diffuse reflectance UV-vis spectroscopy (UV-DR) was used to determine the value of the band gap of the semiconductive materials based on ZnAl-LDHs. The spectra were further processed by tracing the Tauc plots, in order to highlight better the precise value of the band gap (Fig. 6). The values, are, respectively, 3.12 eV for the Ag/ZnAl-LDH (2:1) and of 3.08 eV for the Ag/ZnAl-LDH (3:1) samples.

The values for both samples are close to 3.1 eV, pointing out the potential response of the catalysts when irradiated by visible light.

3.2. Photocatalytic tests

The photocatalytic tests performed on the ZnAl-LDH derived solids highlighted the crucial role of silver in promoting the photocatalytic decomposition of 4-NPh.

On ZnAl-LDH (3:1), the organic compound was not decomposed almost at all during 360 min. of exposure under simulated solar light. This observation is in line with the UV-DR results; the spectrum of this sample is rather flat (not shown). On Ag/ZnAl-LDH (3:1), 87% of 4-NPh was degraded, at room temperature, within 6 h of irradiation by solar light. On the other hand, for Ag/ZnAl-LDH (2:1) catalysts, at the same silver content, the photocatalytic performances are decreased such that only 67% of 4-NPh was decomposed after 360 min of irradiation.

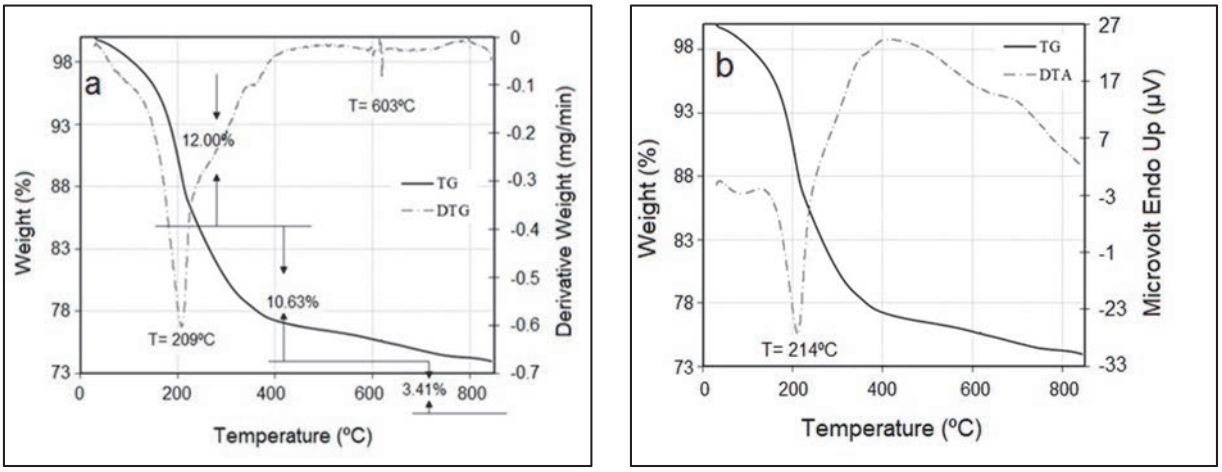

(a) (b)

Fig. 5. The TG/DTG results of (a) Ag/ZnAl-LDH (2:1) and (b) Ag/ZnAl-LDH (3:1)

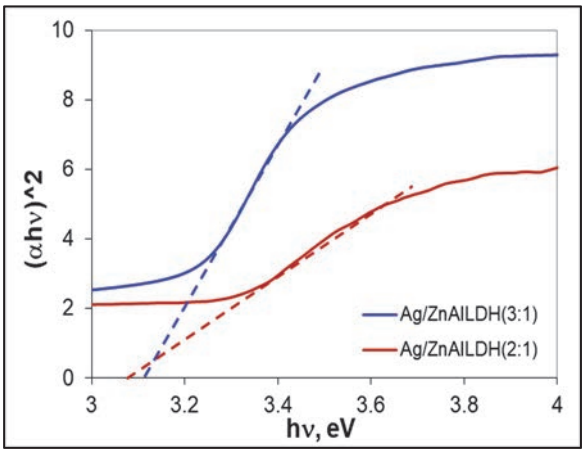

Fig. 6. The Tauc plots of the studied Ag-containing LDHs photocatalysts

This highlights the importance of the LDHs composition (e.g. Zn/Al ratio) in establishing the photocatalyst efficiency. Hence, Ag/ZnAl-LDH (3:1) photocatalyst is the most efficient photocatalytic formulation and its behavior, in terms of conversion degree of 4-NPh evolution in time, is given in Figure 7a and 7b. The conversion values X from Fig. 7a were fitted to a second degree order as a function on irradiation time, with a correlation degree of R^2 = 0.9892 (Eq. 2):

$$X = -0.0005t^2 + 0.386t = 7.2865 \quad (2)$$

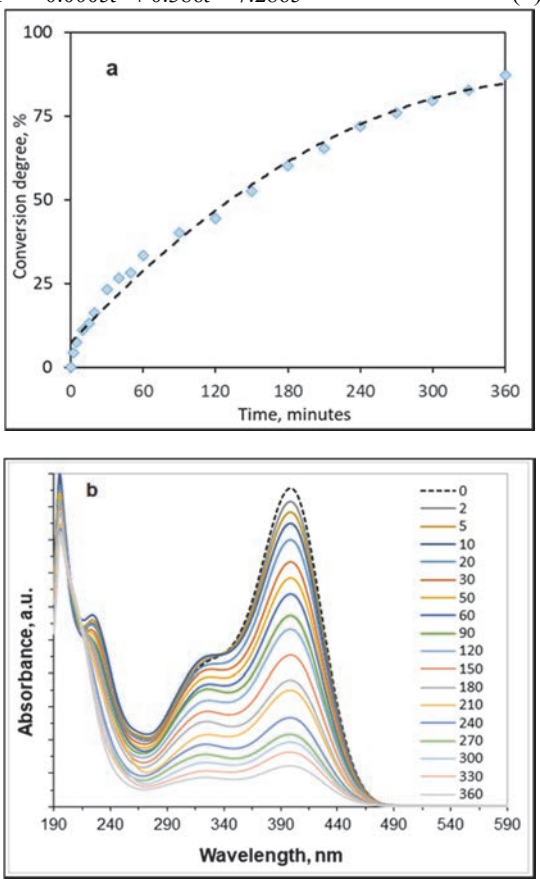

Fig. 7. (a) Photocatalytic conversion as a function of time on the Ag/ZnAl-LDH (3:1), (b) The corresponding UV-Vis response spectra of 4-NPh conversion for an initial concentration of 4 NPh solution: 0.025 g L^{-1}; photocatalyst concentration: 1g L^{-1})

The main peak from 399 nm used to measure the 4-NPh decreases dramatically in each step, corresponding to 33% after 60 min, 44% within 120 min and 87%, after 6 h of solar irradiation.

It is also important to note that bare AgNPs were further tested, using similar experimental conditions (not shown). Results show that the photocatalytic efficiency of nano-sized Ag under solar light is much lower (~ 37%). These results show the importance of the heterostructure formulation between Ag and Zn based LDHs. For Ag/ZnAl-LDH (3:1) that performed as the most efficient catalyst, the turnover number (TON) of the catalytic reaction versus the irradiation time was calculated as the amount of 4-NPh decomposed per gram of catalyst and per hour, using the equation (Eq. 3):

$$TON = C_o * X * 60 / (100 * t) \quad (3)$$

where: TON – turnover number, (h^{-1}), C_o – initial concentration of 4-NPh (0.025 g L^{-1}), X – conversion degree at time t (%), t – irradiation time (min), photocatalyst concentration 1 g L^{-1}.

The evolution of the turnover number as a function of time is given in Fig. 8.

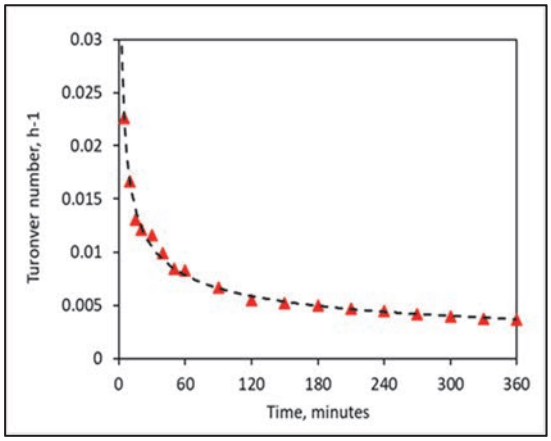

Fig. 8. The yield the 4-NPh decomposition as a function of time for Ag/ZnAl-LDH (3:1)

The results indicate that the turnover number, showing that the efficiency of the photoactive catalytic sites, follows a rapid decrease with irradiation time and the results fitted to the following equation (Eq. 4):

$$TON = 0.0435 * t^{-0.148} \quad (4)$$

After the first hour of illumination, the rate reaches almost a quarter of the initial value. Then, the decrease of the TON is slower. Between 120-360 minutes of photoreaction, the TON values decrease is almost linear. For 210, 240 and 270 minutes of irradiation, the TON value are quite close to each other (0.0046-0.0042 h^{-1}). Therefore, the time value of 210 minutes could be considered the time value marking an important deactivation of the photocatalyst.

The photocatalysis data were fitted to a pseudo-first order reaction kinetics given by the equation (Eq. 5) where k is the reaction rate constant.

$$\ln \frac{C_t}{C_o} = -kt \quad (5)$$

The results (see Fig. 9) confirm the validity of the pseudo-first reaction order in the 4-NPh photocatalytic degradation, in line with the previous reported literature data (Zhang et al., 2018).

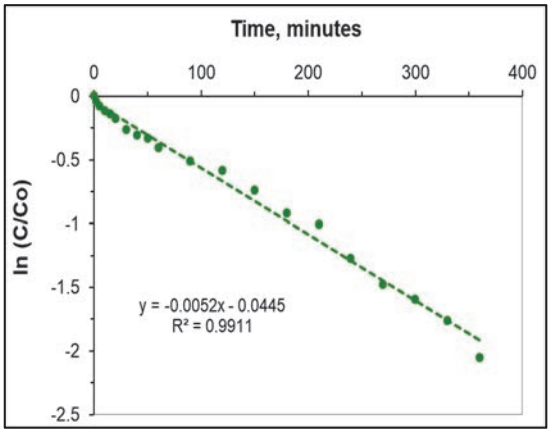

Fig. 9. Pseudo-first order kinetics of 4-NPh decomposition on Ag/ZnAl-LDH (3:1)

4. Conclusions

Heterostuctures of Ag/ZnAl-LDHs were successfully obtained by the reconstruction in aqueous silver nitrate solution of the mixed oxides resulted by the calcination, at 550ºC, of ZnAl (2:1) and ZnAl-LDHs (3:1). The structural investigations performed by XRD shown the formation of the LDH structure by the partial structure reconstruction, while some zinc oxide exists after the re-construction. The FTIR spectra confirm the reconstruction of the LDHs through the presence of characteristic peaks due to CO_3^{2-}, while Ag-O bonds are also detected.

SEM and TEM results reveal that the catalysts are formed of large plate-like nanoparticles of LDHs while nanoparticles of Ag that are deposited on ZnAl-LDH surface (average diameter ~ 7 nm). The values of the band gaps of the Ag/ZnAl-LDH photocatalysts was close to 3.1 eV, revealing that the Ag/LDHs heterostructures can harvest the solar light. The photocatalytic tests showed that the undoped ZnAl-LDH is inactive in the 4-NPh decomposition under simulated solar light. The most active catalyst was Ag/ZnAl-LDH (3:1), with a 4-NPh decomposition degree of 87% after 6 h of solar irradiation. A pseudo-first order kinetics was fitted to describe the experimental data.

Acknowledgements

Diana Gilea acknowledges the financial support of EIT-RM grant for Ph.D. students of ICEEM09.

References

Akhtar M.J., Ahamed M., Kumar S., Khan M.M., Ahmad J., Alrokayan S. A., (2012), Zinc oxide nanoparticles selectively induce apoptosis in human cancer cells through reactive oxygen species, *International Journal of Nanomedicine*, **7**, 845-857.

Balcomb B., Singh M., Singh S., (2015), Synthesis and characterization of layered double hydroxides and their potential as nonviral gene delivery vehicles, *Chemistry Open*, **4**, 137-145.

Bîrsanu M., Puscasu M., Gherasim C., Carja G., (2013), Removal of two industrial dyes from aqueous solutions using hydrotalcite-like anionic clays and their derived mixed oxides as highly efficient photocatalysts, *Environmental Engineering and Management Journal*, **12**, 923-928.

Bora L.V., Mewada R.K., (2017), Visible/solar light active photocatalysts for organic effluent treatment: Fundamentals, mechanisms and parametric review, *Renewable and Sustainable Energy Reviews*, **76**, 1393-1421.

Boumaza A., Favaro L., Ledion J., Sattonnay G., Brubach J.B., Berthet P., Huntz A.M., Roy P., Tetot R., (2009), Transition alumina phases induced by heat treatment of boehmite: An X-ray diffraction and infrared spectroscopy study, *Journal of Solid State Chemistry*, **182**, 1171-1176.

Carja G., Grosu E.F., Mureseanu M., Lutic D., (2017), A family of solar-light responsive photocatalysts obtained by Zn2+Me3+(Me=Al/Ga)LDHs doped with Ga2O3 and In2O3 and their derived mixed oxides: A case study of Phenol/p-Nitrophenol decomposition, *Catalysis Scence and Technol*ogy, **7**, 5402-5412.

Carja G., Grosu, E.F., Petrarean, C., Nichita, N., (2015), Self-assemblies of plasmonic gold/layered double hydroxides with highly efficient antiviral effect against the hepatitis B virus, *Nano Research*, **8**, 3512-3523.

Chen C., Gunawan P., Lou (David) X.W., Xu R., (2012), Silver nanoparticles deposited layered double hydroxide, Nanoporous coatings with excellent antimicrobial activities, *Advanced Functional Materials*, **22**, 780-787.

Elhalil A., Farnane, M., Machrouhi A., Mahjoubi F. Z., Elmoubarki R., Tounsadi H., Abdennouri M., Barka N., (2018), Effects of molar ratio and calcination temperature on the adsorption performance of Zn/Al layered double hydroxide nanoparticles in the removal of pharmaceutical pollutants, *Journal of Science: Advanced Materials and Devices*, **3**, 188-195.

Gilea D., Radu T., Muresanu M., Carja G., (2018), Plasmonic photocatalysts based on silver nanoparticles – layered double hydroxides for efficient removal of toxic compounds using solar light, *Applied Surface Science*, **444**, 407-413.

Girish Kumar S., Koteswara Rao K.S.R., (2015), Zinc oxide based photocatalysis: tailoring surface-bulk structure and related interfacial charge carrier dynamics for better environmental applications, *RSC Advances*, **5**, 3306-3351.

Islam D.A., Borah D., Acharya H., (2014), Controlled synthesis of monodisperse silver nanoparticles supported layered double hydroxides catalyst, *RSC Advances*, **5**, 13239-13245.

Khaki M.R.D., Shafeeyan M.S., Raman A.A.A., Daud W.M.A.W., (2018), Evaluating the efficiency of nano-sized Cu doped TiO_2/ZnO photocatalyst under visible light irradiation, *Journal of Molecular Liquids*, **258**, 354-365.

Mishra G., Dash B., Pandey S., (2018), Layered double hydroxides: A brief review from fundamentals to application as evolving biomaterials, *Applied Clay Science*, **153**, 172-186.

Rafiq M., Siddiqui H., Adil S.F., Assal M.E., Roushown A., Al-Warthan A., (2013), Synthesis and characterization of silver oxide and silver chloride nanoparticles with high thermal stability, *Asian Journal of Chemistry*, **25**, 3405-3409.

Rocha J., del Arco M., Rives V., Ulibarri M. A. (1999) Reconstruction of layered double hydroxides from calcined precursors: a powder XRD and 27Al MAS NMR study, *Journal of Materials Chemistry*, **9**, 2499-2503.

Seftel E.M., Cool P., Lutic D., (2013), Mg–Al and Zn–Fe layered double hydroxides used for organic species storage and controlled release, *Materials Science and Engineering C*, **33**, 5071-5078.

Seftel E.M., Puscasu M., Mertens M., Cool P., Carja G., (2015), Photo-responsive behavior of γ-Fe2O3 NPs embedded into ZnAlFe-LDH matrices and their catalytic efficiency in wastewater remediation, *Catalysis Today*, **252**, 7-13.

Sharma R.K., Ghosen R., (2014), Synthesis and characterization of nanocrystalline zinc aluminate spinel powder by sol–gel method, *Ceramics International*, **40**, 3209-3214.

Tauc J. (1968), Optical properties and electronic structure of amorphous Ge and Si, *Materials Research Bulletin*, **3**, 37-46.

Valcheva-Traykova M.L., Davidov N.P., Weiss A.H., (1993), Thermal decomposition of Mg, Al-hydrotalcite material, *Journal of Materials Science*, **28**, 2157-2162.

Waterhouse G.I.N., Bowmaker G.A., Metson J.B., (2001), The thermal decomposition of silver (I, III) oxide: A combined XRD, FT-IR and Raman spectroscopic study, *Physical Chemistry Chemical Physics*, **3**, 3838-3845.

Xu Z.P., Zeng Q.H., Lu G.Q., Yu A B., (2006), Inorganic nanoparticles as carriers for efficient cellular delivery, *Chemical Engineering Science*, **61**, 1027-1040.

Zhang G., Hu L., Zhao R., Su R., Wang Q., Wang P., (2018), Microwave-assisted synthesis of ZnNiAl-layered double hydroxides with calcination treatment for enhanced PNP photo-degradation under visible-light irradiation, *Journal of Photochemistry and Photobiology A: Chemistry*, **356**, 633-641.

Zhao X., Zhang F., Xu S., Evans D.G., Duan X., (2010), From layered double hydroxides to ZnO-based mixed metal oxides by thermal decomposition: transformation mechanism and UV-blocking properties of the product, *Chemistry of Materials*, **22**, 3933-3942.